AGU PUBLICATIONS

Geophysical Research Letters

RESEARCH LETTER
10.1002/2014GL062943

Key Points:
- A novel high-resolution airborne sensor is flown
- Both red and far red Sun-induced fluorescence signals are accurately quantified
- Red and far red fluorescence tracks variations in photosynthetic efficiency

Supporting Information:
- Text S1–S4, Tables S1 and S2, and Figure S1

Correspondence to:
M. Rossini,
micol.rossini@unimib.it

Citation:
Rossini, M., et al. (2015), Red and far red Sun-induced chlorophyll fluorescence as a measure of plant photosynthesis, *Geophys. Res. Lett.*, *42*, doi:10.1002/2014GL062943.

Received 23 DEC 2014
Accepted 18 FEB 2015
Accepted article online 20 FEB 2015

Red and far red Sun-induced chlorophyll fluorescence as a measure of plant photosynthesis

M. Rossini[1], L. Nedbal[2], L. Guanter[3], A. Ač[4], L. Alonso[5], A. Burkart[2], S. Cogliati[1], R. Colombo[1], A. Damm[6], M. Drusch[7], J. Hanus[4], R. Janoutova[4], T. Julitta[1], P. Kokkalis[8], J. Moreno[5], J. Novotny[4], C. Panigada[1], F. Pinto[2], A. Schickling[2], D. Schüttemeyer[7], F. Zemek[4], and U. Rascher[2]

[1]Remote Sensing of Environmental Dynamics Lab., DISAT, Università degli Studi Milano-Bicocca, Milan, Italy, [2]Institute of Bio- and Geosciences-2: Plant Sciences, Forschungszentrum Jülich GmbH, Jülich, Germany, [3]Helmholtz Center Potsdam, German Research Center for Geosciences, Potsdam, Germany, [4]Global Change Research Centre AS CR, Brno, Czech Republic, [5]Department of Earth Physics and Thermodynamics, University of Valencia, Burjassot, Spain, [6]Remote Sensing Laboratories, University of Zurich, Zurich, Switzerland, [7]European Space Agency, ESTEC, Noordwijk, Netherlands, [8]Institute for Astronomy, Astrophysics, Space Applications and Remote Sensing, National Observatory of Athens, Athens, Greece

Abstract Remote estimation of Sun-induced chlorophyll fluorescence emitted by terrestrial vegetation can provide an unparalleled opportunity to track spatiotemporal variations of photosynthetic efficiency. Here we provide the first direct experimental evidence that the two peaks of the chlorophyll fluorescence spectrum can be accurately mapped from high-resolution radiance spectra and that the signal is linked to variations in actual photosynthetic efficiency. Red and far red fluorescence measured using a novel airborne imaging spectrometer over a grass carpet treated with an herbicide known to inhibit photosynthesis was significantly higher than the corresponding signal from an equivalent untreated grass carpet. The reflectance signal of the two grass carpets was indistinguishable, confirming that the fast dynamic changes in fluorescence emission were related to variations in the functional status of actual photosynthesis induced by herbicide application. Our results from a controlled experiment at the local scale illustrate the potential for the global mapping of terrestrial photosynthesis through space-borne measurements of chlorophyll fluorescence.

1. Introduction

Photosynthesis is the process in which plants utilize sunlight to transform carbon dioxide and water into carbohydrate macromolecules. Photosynthesis is the foundation of nearly all energy available for life on Earth; hence, understanding how photosynthesis responds to the environment is important for improving plant production and for coping with global change [*Flexas et al.,* 2012]. Photosynthesis is an actively regulated process with a significant capacity to adjust for dynamic environmental conditions [*Horton and Ruban*, 1992; *Ruban et al.,* 2007]. These adjustments can occur in the short-term, triggering reversible modifications to the fate of the light absorbed by green vegetation. Under favorable environmental conditions, plants use the majority of absorbed light for photosynthetic conversion, and only a small part is emitted as chlorophyll fluorescence or nonradiatively as heat [*Demmig-Adams and Adams*, 2000]. When vegetation experiences suboptimal growing conditions, it reduces its photosynthetic efficiency as a consequence of different protective mechanisms or plant tissue damages. Since light reactions of photosynthesis, fluorescence, and heat dissipation occur in competition, variation in the efficiency of one process affects the efficiencies of the others. This link forms the rationale for the use of fluorescence to infer the actual functional state of the photosynthetic apparatus since photosynthetic efficiency affects the efficiency of fluorescence emission.

Compared to fluorescence emission, surface reflectance typically used in remote sensing applications reflects only late responses to variations in environmental conditions related to changes in plant pigment composition; therefore, surface reflectance cannot capture early photosynthesis responses that are more dynamic [*Grace et al.,* 2007]. Under natural sunlight illumination, the amount of chlorophyll fluorescence emitted by vegetation represents a tiny fraction of the radiation reflected by a plant in the red and near-infrared part of the electromagnetic spectrum. However, the fluorescence signal can be quantified from space-based, high-resolution spectrometers exploiting dark regions of the atmospheric and solar absorption spectra where the incident irradiance is strongly reduced.

The chlorophyll fluorescence spectrum emitted by plants is characterized by two broadband peaks centered in the red (685 nm, F_R) and far red (740 nm, F_{FR}) spectral regions. Thus, far, most published papers report Sun-induced chlorophyll fluorescence measured by exploiting either telluric O_2 bands or solar Fraunhofer lines in the near-infrared region, proving the feasibility to detect the F_{FR} signal from tower [*Cheng et al.,* 2013; *Meroni et al.,* 2011; *Moya et al.,* 2004; *Rossini et al.,* 2010], aircraft [*Panigada et al.,* 2014; *Rascher et al.,* 2009; *Zarco-Tejada et al.,* 2012], and satellite platforms [*Frankenberg et al.,* 2011; *Guanter et al.,* 2012, 2014; *Joiner et al.,* 2013] with different levels of accuracy. Only a few studies have dealt with the estimation of F_R from tower platforms [*Cheng et al.,* 2013; *Daumard et al.,* 2010; *Fournier et al.,* 2012] or airborne point sensors based on interference filters [*Moya and Flexas*, 2012] because the majority of available instruments have a resolution that is too low to properly retrieve F_R and resolve the width of the narrow O_2 B band.

The *HyPlant* sensor developed by the Forschungszentrum Jülich (Germany) in cooperation with the company Specim Spectral Imaging Ltd (Finland) and used in the present study is, to the best of our knowledge, the only currently available and operational airborne sensor with a subnanometer spectral resolution in the 670 to 780 nm spectral region. Thus, the HyPlant sensor offered an unparalleled opportunity to estimate not only F_{FR} in the O_2 A-band but also F_R fluorescence in the much narrower O_2 B band from an airborne platform. This high-performance imaging spectrometer has been developed within the framework of European Space Agency's (ESA's) Fluorescence Explorer (FLEX) mission Phase A activities and represents an airborne demonstrator for the FLEX mission.

In this letter we present the results of a dedicated experiment designed to cause traceable variations in photosynthetic efficiency in a short time period without affecting canopy structure and the composition of plant biochemical compounds. The HyPlant sensor was flown over two grass carpets to evaluate the potential of Sun-induced fluorescence to detect changes in photosynthetic efficiency induced by a stress factor applied to one of them. The stress factor we applied in this study was the herbicide 3-(3′,4′-dichlorophenyl)-1,1-dimethylurea (DCMU), which is known to bind selectively to photosystem II (PSII) and block its reoxidation by the plastoquinone pool [*Van Rensen*, 1989]. Thus, the DCMU-treated grass cannot perform the linear photosynthetic electron transport, and the resulting excess energy causes an increase of chlorophyll fluorescence emission. This increase in chlorophyll fluorescence emission is expected because DCMU is known to inhibit also the nonradiative dissipation of excitation energy through the reduction of the energy-dependent nonphotochemical quenching generated by the photosynthetic electron transport [*Ruban et al.,* 1992]. In contrast, binding DCMU to PSII does not influence the leaf pigment composition in the short-term; thus, we do not expect reflectance to be affected by the herbicide treatment during this experiment. Other stress factors that may occur under natural environmental conditions generally induce a different response of fluorescence emission. Natural stress factors induce a reduction of photosynthetic efficiency but typically increase nonphotochemical quenching generally resulting in a decline in fluorescence emission. However, the response of fluorescence to different stress factors is not unique and its interpretation could not be straightforward due to the cooccurrence of the nonphotochemical quenching during chlorophyll fluorescence [*Porcar-Castell et al.,* 2014; *Roháček et al.,* 2008].

2. Experiment Description

2.1. Experiment Preparation

The experiment took place in the study site Bíly Kriz (18.54°E, 49.49°N, 860 m above sea level). Two commercially produced grass carpets (12 × 12 m each) composed of *Festuca rubra, Lolium repenne,* and *Poa pratensis* were treated with DCMU (Figure 1). One of the grass carpets was treated on 5 September 2012 in the early morning by DCMU diluted to 10^{-5} M in 1% ethanol/water and on 9 September with an herbicide concentration that was 10 times higher (10^{-4} M DCMU). On both days, the control carpet was treated at the same time with 1% ethanol/water without the herbicide. Effects of the DCMU application on the biochemistry of leaves were assessed through chlorophyll and carotenoid concentration extractions. Details about the pigment extractions are reported in the supporting information.

2.2. Ground Measurements of High-Resolution Top-of-Canopy Radiance and Reflectance

Measurements of top-of-canopy radiances leaving the grass carpet were performed from a distance of 4.2 m using an Analytical Spectral Devices Inc. (ASD) field spectrometer (ASD FieldSpec-3, Boulder, CO, USA) that was

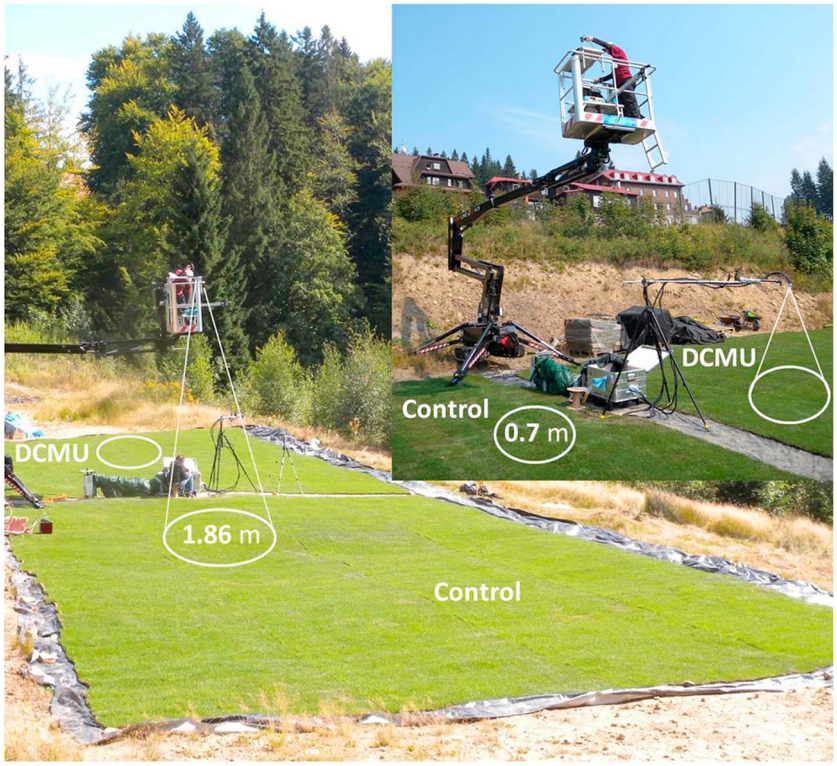

Figure 1. Experimental site with a treated (DCMU) and an untreated (control) grass carpet. Ground spectral data were collected in circular areas (approximately 1.86 m in diameter) in both the treated (3-(3′,4′-dichlorophenyl)-1,1-dimethylurea (DCMU)) and the control plot using an ASD field spectrometer. The ASD instrument was installed on a hydraulic platform that allowed moving the fore optic and measuring both plots sequentially. Additional high-resolution spectral measurements were collected (inlet at the top right corner) by a Multiplexer Radiometer/Irradiometer consisting of two portable OceanOptics spectrometers equipped with optical fibers and mounted on a mobile arm swinging over both plots. The measured area covers a circular area (approximately 0.7 m in diameter) of both grass carpets.

positioned alternatingly over the DCMU-treated and the control grass carpet using a small hydraulic movable platform. Hemispherical-Conical Reflectance Factor [*Schaepman-Strub et al.,* 2006] was computed in the spectral range 350 to 2,500 nm using measurements of a white reference calibrated panel (Spectralon, LabSphere, USA) to estimate the incident irradiance. With a field of view of 25°, the diameter of each acquisition was about 1.8 m. Simultaneously, the grass leaving radiances were measured with an automatic system named Multiplexer Radiometer/Irradiometer [*Cogliati*, 2011] from a distance of 1.6 m corresponding to a ground sampling area of 0.7 m in diameter sequentially positioned on the DCMU-treated and the control grass carpet. The system hosts two portable spectrometers (HR4000, OceanOptics, USA) characterized by different spectral resolutions, including a spectrometer specifically intended for F_{FR} estimation (spectral range 700 to 800 nm and full width at half maximum (FWHM) of 0.1 nm). An optical multiplexer (MPM-2000, OceanOptics, USA) is used to switch between a channel measuring the downwelling irradiance using a cosine-response optic (cc3, OceanOptics, USA), a 25° downward looking bare fiber for the measurement of the upwelling radiance and a "blind" channel for the dark current measurement. Reflectance measurements derived from the ASD spectrometer were used to compute the normalized difference vegetation index (NDVI) [*Rouse et al.,* 1974].

F_{FR} was estimated from the high-resolution OceanOptics spectrometer using the spectral fitting method [*Meroni et al.,* 2010] and assuming a linear variation of reflectance and F_{FR}. The apparent fluorescence yield (Fy_{FR}) was also computed as the ratio between F_{FR} and the incident photosynthetically active radiation (see supporting information for a detailed description of applied methods).

2.3. Airborne Hyperspectral Imagery Acquisition and Processing

Airborne images were acquired on 5 and 9 September 2012 with the HyPlant sensor consisting of an imager specifically designed for fluorescence estimation covering the wavelength range 670 to 780 nm with 1024

spectral bands with a FWHM of 0.25 nm and a sampling interval of 0.11 nm. This module has a signal-to-noise ratio with full scale signal of 240. The sensor was flown 6 times over the study area, 4 times on 5 September and 2 times on 9 September. The data acquisition time was between 11:01 and 15:25 Central European Solar Time (CEST) with a flight path direction oriented south to north. Details about data acquisition times and flight geometries are reported in the supporting information. The flights were conducted at an average altitude of 600 m above ground level corresponding to a pixel size of about 1 m.

F_{FR} and F_R have been estimated from HyPlant using spectral fitting windows sampling different parts of the fluorescence spectrum (e.g., 672–702 nm, 725–759 nm, and 740–780 nm). The forward model for the retrieval represents at-sensor radiance spectra as the combination of the spectral contributions of surface reflectance, fluorescence, and atmospheric radiative transfer. Surface reflectance is modeled by means of third-order polynomials in wavelength characterizing the spectrally smooth variations of reflectance within the fitting windows, whereas fluorescence is represented by a fixed spectral shape scaled by a constant factor accounting for the intensity of the signal. Regarding the modeling of atmospheric radiative transfer effects (namely, the atmospheric transmittance between the top-of-atmosphere, the target, and the sensor), two different approaches have been tested: (i) the singular vector decomposition as described in *Guanter et al.* [2013] and *Joiner et al.* [2013] that represents spectral effects of atmospheric absorption and scattering processes by a series of spectral functions (singular vectors); (ii) a physically based approach that incorporates explicit atmospheric radiative transfer modeling using the MODTRAN5 atmospheric radiative transfer code. MODTRAN5 is constrained with a series of parameters describing the HyPlant observation geometry, whereas parameters that drive atmospheric radiative transfer in each fitting window are inverted together with the polynomial coefficients and the fluorescence intensity parameter following an iterative minimisation process (see supporting information for details).

The fluorescence retrievals with the two methods yielded similar results regarding the effect of DCMU application on both F_R and F_{FR} values. Based on image visual inspection and on the comparison between ground and airborne F_{FR} estimates, we selected the retrievals based on physical radiative transfer modeling for F_{FR}, and the statistical approach for F_R. The apparent fluorescence yield was also computed as the ratio between F_R and F_{FR} and the incident photosynthetically active radiation at the time of the overpass. HyPlant reflectance measurements were then used to compute different vegetation indices, results obtained using NDVI are reported in this contribution.

3. Results and Discussion

The night before the first campaign date (5 September), we applied the herbicide by spraying at a concentration of 10^{-5} M, which is known to inhibit reoxidation of PSII when applied to isolated chloroplasts or algae [*Krause and Weis*, 1984]. The application to leaves was securely in the range in which no short-term pigment destruction can occur. Indeed, we found no statistical difference (according to Student's *t* test) between the DCMU-treated and control plots in the leaf pigment concentration evaluated through leaf chemical extractions (see supporting information). Accordingly, classical vegetation indices related to plant green biomass or leaf chlorophyll content did not markedly differ between the two grass carpets. As a reference, we show the map of the NDVI computed from the midday flight is shown in Figure 2a. Instead, the far red chlorophyll fluorescence estimated from the HyPlant radiance data (F_{FR}, Figure 2b) was higher in the herbicide-treated plot compared to the control plot. The enhancement was relatively small because the herbicide concentration that penetrated from leaf surface and roots to chloroplasts of the grass plants was not saturating. Nevertheless, we also saw the expected fluorescence emission dynamics in the diurnal pattern of the average fluorescence values extracted from the maps with an intensity generally proportional to the incident radiance, being maximum around solar noon and lower in the morning and afternoon (Figure 3b). The afternoon (15:25 CEST) values were particularly low because of the lower incident irradiance, which reduced the rate of the photosynthetic charge separation, thus reducing the Q_A primary acceptor in PSII [*Krause and Weis*, 1984]. The fluorescence signal is dependent on the incident irradiance, but the computation of the apparent fluorescence yield (Figure 3c) allows us to remove this dependence.

The F_R maps (Figure 2c) we obtained from the imaging airborne sensor showed that plants with photosynthesis impaired by DCMU application had higher F_R values than those measured on the control plot. Furthermore, F_R exhibited the expected diurnal dynamic (Figure 3b) with values proportional to the incident irradiance as

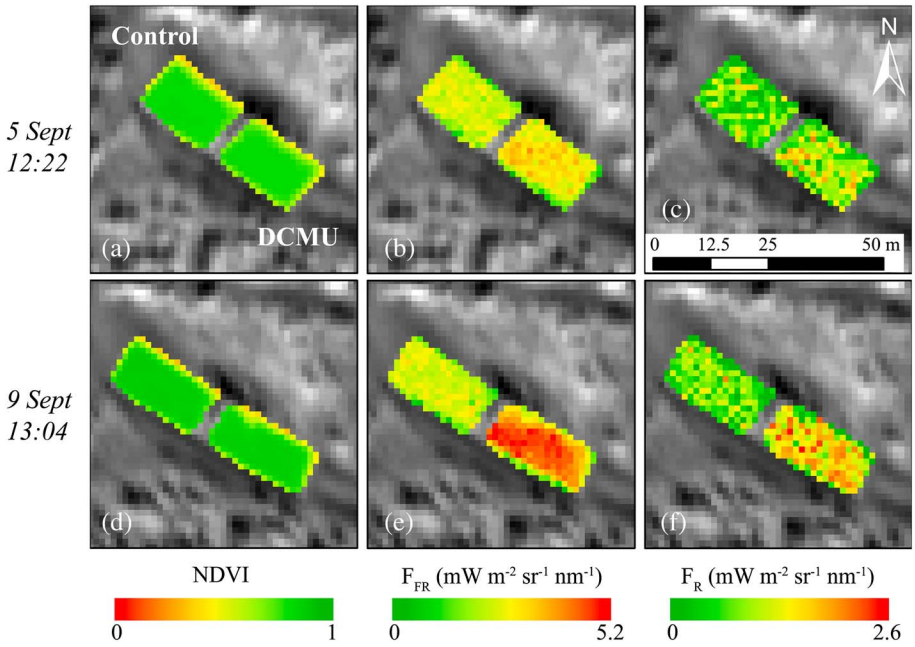

Figure 2. Control (left) and DCMU-treated (right) grass plots in airborne images. (a, d) Normalized difference vegetation index (NDVI). (b, e) Far red chlorophyll fluorescence (F_{FR}). (c, f) Red chlorophyll fluorescence emission (F_R). The dates and hours (CEST) on the left indicate the data acquisition time.

already observed for F_{FR} and higher values in the herbicide-treated plot compared to the control plot for all four acquisition times, confirming the relevance of the F_R signal to track the photosynthetic efficiency as well as the validity of the retrieval algorithms used here. It is worth noting that F_R maps are characterized by a higher within-treatment variability compared to F_{FR} probably because of the higher retrieval noise associated to the shallower solar and atmospheric lines in the window from 670 to 690 nm.

Using the next flight opportunity, we applied a 10 times higher herbicide concentration (10^{-4} M) and collected airborne imageries on 9 September at 13:04 and 15:13 CEST. The higher herbicide concentration significantly increased the difference between fluorescence emission from the herbicide-treated and control plots (Figures 2e and 2f), with maximum differences at midday (Figure 3b), while NDVI differed only slightly between the two plots (Figure 2d). NDVI generally showed a moderate increase from 5 to 9 September (Figure 3a). This increase was slightly higher for the control plot compared to the DCMU-treated one, indicating that the prolonged action by the earlier low-dose application of the herbicide lead to a slowdown in plant productivity and related biomass development that cannot, however, explain the increased fluorescence values.

Regarding fluorescence, the second application of DCMU caused an increase of F_{FR} up to 5 mW m^{-2} sr^{-1} nm^{-1} on 9 September. This value is more than the double of the values measured on both the treated and the control plots on 5 September and more than the double of the value measured on the same day in the control plot. A similar increase was observed also for F_R with values up to 2 mW m^{-2} sr^{-1} nm^{-1} in the herbicide-treated plot, a value 2 times higher than that measured in the control plot.

The apparent fluorescence yield (Fy) shows a more stable diurnal course on the first day (5 September) (Figure 3c) and a time course inversely related to the incident irradiance on 9 September, with minimum values around midday. This behavior could indicate that the grass carpet is regulating the efficiency of the dissipation pathways in response to variations in incident radiation. However we cannot exclude a superimposed effect of changing illumination geometry caused by changing Sun position during the day, which could also explain the slight changes in NDVI observed along the two days (Figure 3a).

The ratio F_{FR}/F_R computed on the control grass shows values ranging between 2.8 and 3.5. These values are higher than those generally observed at leaf level although the comparison with leaf values is not straightforward because the values reported in the literature are often obtained using artificial light sources with an excitation spectrum different from the solar one. We attribute these higher values at canopy level to reabsorption of F_R by

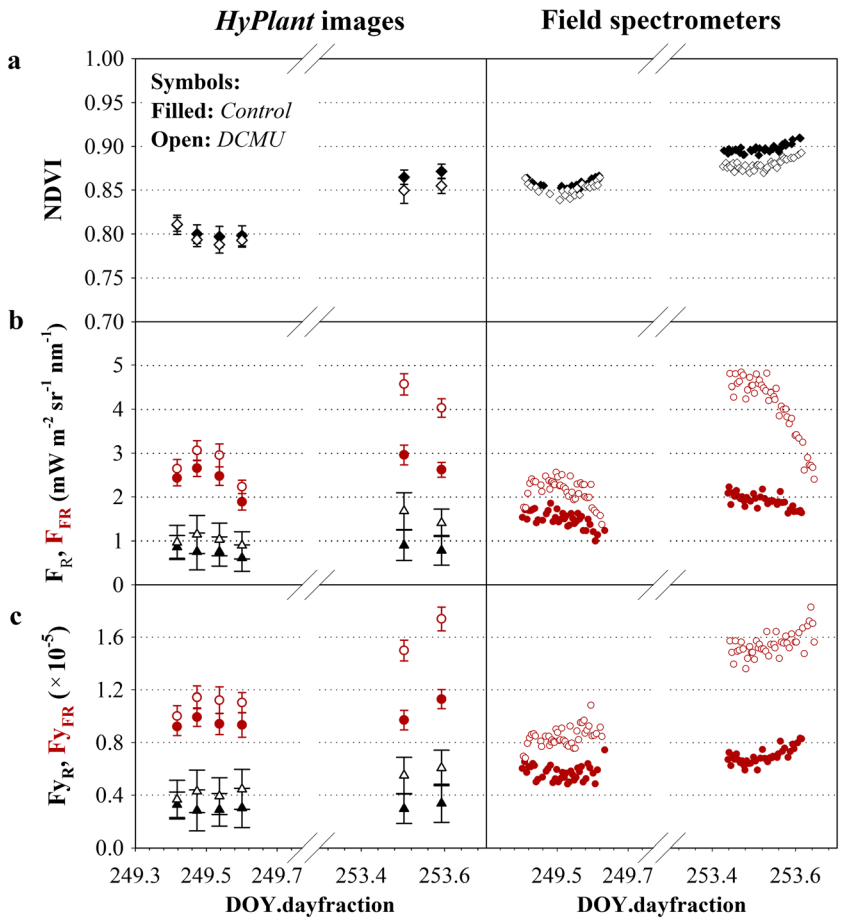

Figure 3. Time courses of red (triangle symbol) and far red fluorescence (circle symbol), respective fluorescence yields, and normalized difference vegetation index (NDVI) (diamond symbol) obtained from HyPlant images (left column) and in situ field spectroscopy data (right column). (a) NDVI. (b) Fluorescence emission in the red (F_R) and far red (F_{FR}) region. (c) Apparent fluorescence yield in the red (Fy_R) and far red (Fy_{FR}) region. The NDVI was measured in situ using an ASD spectrometer, F_{FR} and Fy_{FR} were derived from high-resolution OceanOptics spectrometer data. Filled symbols represent the values measured over the control plot and open symbols those measured over the DCMU-treated plot during 5 September (day of year 249) and 9 September (day of year 253). The error bars shown for the airborne measurements correspond to +1/−1 standard deviation of values extracted from HyPlant images for each plot and flight.

photosynthetic pigments within the canopy causing a rise of the F_{FR}/F_R ratio compared to the leaf level. Retrieval biases at either spectral region cannot be discarded either.

With respect to the control, the magnitude of the F_{FR} signal increased up to 20% and 55% for the low- and high-concentration treatment, respectively, while it increased up to 50% and 85% in the red region. When we interpret these results, we should consider that F_R and a major portion of F_{FR} originate from PSII at ambient temperature and that only a small fraction of fluorescence from Photosystem I (PSI) contributes to F_{FR} [*Lichtenthaler and Rinderle*, 1988]. DCMU blocks electron transport from PSII to PSI when it binds to site of the electron acceptor quinone in PSII, giving rise to a considerable increase in the F_R and F_{FR} emission, as was previously observed in leaf-level fluorescence measurements [*Kim et al.,* 2001; *Lichtenthaler and Miehé*, 1997]. The rate increases of F_R were higher compared to those of F_{FR}, owing to inhibition of the electron transport in the photosynthetic apparatus [*Kim et al.,* 2001; *Lichtenthaler et al.,* 1996].

We validate reflectance and F_{FR} results obtained from HyPlant by using spectral measurements collected on the ground with state-of-the-art field spectrometers. Proper validation of F_R values was not possible because the spectrometers used on the ground did not have a high enough spectral resolution to resolve sufficiently the absorption features in the O_2 B band. We detected the increased F_{FR} with top-of-canopy measurements, and the surface reflectance was almost unaffected by the herbicide treatment (Figures 3a–3c, right column).

F_{FR} measurements on the ground reflect the great range of variation extracted from the airborne F_{FR} maps, which are linearly related with a determination coefficient of 0.95. Values from HyPlant are slightly higher than those from field spectrometer and particularly for low fluorescence values.

4. Conclusions

The results we present in this manuscript are the first experimental proof that the quantitative estimation of both red and far red fluorescence is possible through high spectral resolution remote sensing measurements in the 670 to 780 nm spectral region, confirming the scientific maturity of the ESA FLEX mission concept and objectives. An airborne instrument with specifications and performance comparable to the actual FLEX high-resolution spectrometer was flown over two grass carpets, one treated by a herbicide known to inhibit photosynthesis and selectively intensify fluorescence emission. A significant increase of both red and far red fluorescence was detected on the treated grass carpet from the airborne platform, while the reflectance signals of the control and treated grass were indistinguishable.

This result proves that the quantitative estimation of F_{FR} and, for the first time ever, F_R is possible from an airborne platform and showed that both F_R and F_{FR} provide information that can help in the interpretation of the processing modulating the photosynthetic activity of vegetation.

Acknowledgments

Data presented in this contribution were acquired in the frame of the HyFLEX campaign funded by the European Space Agency (ESA) (ESA ESTEC RFQ-3-13566/12/NL/LF). Algorithms for fluorescence retrieval have been developed in the frame of the FLEX/S3 Tandem Mission Performance Analysis and Requirements Consolidation Study funded by ESA (ESA ESTEC RFQ 3-13397/11/NL/CBi). HyPlant was developed by a large-scale investment grant of the Helmholtz Association. We thank Damien Markulin for his support during data collection and Kristýna Večeřová for leaf pigment analysis. Data used in this contribution are available upon request to the corresponding author.

The Editor thanks Christian van der Tol and an anonymous reviewer for their assistance in evaluating this paper.

References

Cheng, Y.-B., E. Middleton, Q. Zhang, K. Huemmrich, P. Campbell, L. Corp, B. Cook, W. Kustas, and C. Daughtry (2013), Integrating solar induced fluorescence and the photochemical reflectance index for estimating gross primary production in a cornfield, *Remote Sens.*, *5*(12), 6857–6879.

Cogliati, S. (2011), Development of automatic spectrometric systems for proximal sensing of photosynthetic activity of vegetation, PhD thesis, 162 pp., Univ. of Milano-Bicocca, Italy.

Daumard, F., S. Champagne, A. Fournier, Y. Goulas, A. Ounis, J.-F. Hanocq, and I. Moya (2010), A field platform for continuous measurement of canopy fluorescence, *IEEE Trans. Geosci. Remote Sens.*, *48*(9), 3358–3368.

Demmig-Adams, B., and W. W. Adams (2000), Photosynthesis: Harvesting sunlight safely, *Nature*, *403*(6768), 371–374.

Flexas, J., F. Loreto, and H. Medrano (Eds.) (2012), *Terrestrial Photosynthesis in a Changing Environment*, *A Molecular, Physiological and Ecological Approach,* Cambridge Univ. Press, New York.

Fournier, A., F. Daumard, S. Champagne, A. Ounis, Y. Goulas, and I. Moya (2012), Effect of canopy structure on Sun-induced chlorophyll fluorescence, *ISPRS J. Photogramm. Remote Sens.*, *68*, 112–120.

Frankenberg, C., et al. (2011), New global observations of the terrestrial carbon cycle from GOSAT: Patterns of plant fluorescence with gross primary productivity, *Geophys. Res. Lett.*, *38*, L17706, doi:10.1029/2011GL048738.

Grace, J., C. Nichol, M. Disney, P. Lewis, T. Quaife, and P. Bowyer (2007), Can we measure terrestrial photosynthesis from space directly, using spectral reflectance and fluorescence?, *Global Change Biol.*, *13*(7), 1484–1497.

Guanter, L., C. Frankenberg, A. Dudhia, P. E. Lewis, J. Gómez-Dans, A. Kuze, H. Suto, and R. G. Grainger (2012), Retrieval and global assessment of terrestrial chlorophyll fluorescence from GOSAT space measurements, *Remote Sens. Environ.*, *121*, 236–251.

Guanter, L., M. Rossini, R. Colombo, M. Meroni, C. Frankenberg, J.-E. Lee, and J. Joiner (2013), Using field spectroscopy to assess the potential of statistical approaches for the retrieval of Sun-induced chlorophyll fluorescence from ground and space, *Remote Sens. Environ.*, *133*, 52–61.

Guanter, L., et al. (2014), Global and time-resolved monitoring of crop photosynthesis with chlorophyll fluorescence, *Proc. Natl. Acad. Sci. U.S.A.*, doi:10.1073/pnas.1320008111.

Horton, P., and A. V. Ruban (1992), Regulation of photosystem II, *Photosynth. Res.*, *34*(3), 375–385.

Joiner, J., L. Guanter, R. Lindstrot, M. Voigt, A. P. Vasilkov, E. M. Middleton, K. F. Huemmrich, Y. Yoshida, and C. Frankenberg (2013), Global monitoring of terrestrial chlorophyll fluorescence from moderate-spectral-resolution near-infrared satellite measurements: Methodology, simulations, and application to GOME-2, *Atmos. Meas. Tech.*, *6*(10), 2803–2823.

Kim, M. S., J. E. McMurtrey, C. L. Mulchi, C. S. T. Daughtry, E. W. Chappelle, and Y.-R. Chen (2001), Steady-state multispectral fluorescence imaging system for plant leaves, *Appl. Opt.*, *40*(1), 157–166.

Krause, G. H., and E. Weis (1984), Chlorophyll fluorescence as a tool in plant physiology, *Photosynth. Res.*, *5*(2), 139–157.

Lichtenthaler, H. K., and J. A. Miehé (1997), Fluorescence imaging as a diagnostic tool for plant stress, *Trends Plant Sci.*, *2*(8), 316–320.

Lichtenthaler, H. K., and U. Rinderle (1988), Role of chlorophyll fluorescence in the detection of stress conditions in plants, *Crit. Rev. Anal. Chem.*, *19*, 529–585.

Lichtenthaler, H. K., M. Lang, M. Sowinska, F. Heisel, and J. A. Miehe (1996), Detection of vegetation stress via a new high resolution fluorescence imaging system, *J. Plant Physiol.*, *148*(5), 599–612.

Meroni, M., L. Busetto, R. Colombo, L. Guanter, J. Moreno, and W. Verhoef (2010), Performance of spectral fitting methods for vegetation fluorescence quantification, *Remote Sens. Environ.*, *114*(2), 363–374.

Meroni, M., et al. (2011), The hyperspectral irradiometer, a new instrument for long-term and unattended field spectroscopy measurements, *Rev. Sci. Instrum.*, *82*(4, 043106-043101-043109), doi:10.1063/1.3574360.

Moya, I., and J. Flexas (2012), Remote sensing of photosynthesis, in *Terrestrial Photosynthesis in a Changing Environment: A Molecular, Physiological, and Ecological Approach*, edited by F. L. Jaume Flexas and H. Medrano, pp. 219–236, Cambridge Univ. Press, New York.

Moya, I., L. Camenen, S. Evain, Y. Goulas, Z. G. Cerovic, G. Latouche, J. Flexas, and A. Ounis (2004), A new instrument for passive remote sensing: 1. Measurements of sunlight-induced chlorophyll fluorescence, *Remote Sens. Environ.*, *91*(2), 186–197.

Panigada, C., et al. (2014), Fluorescence, PRI and canopy temperature for water stress detection in cereal crops, *Int. J. Appl. Earth Obs. Geoinf.*, *30*, 167–178.

Porcar-Castell, A., E. Tyystjärvi, J. Atherton, C. van der Tol, J. Flexas, E. E. Pfündel, J. Moreno, C. Frankenberg, and J. A. Berry (2014), Linking chlorophyll a fluorescence to photosynthesis for remote sensing applications: Mechanisms and challenges, *J. Exp. Bot.*, *65*(15), 4065–4095, doi:10.1093/jxb/eru191.

Rascher, U., et al. (2009), CEFLES2: The remote sensing component to quantify photosynthetic efficiency from the leaf to the region by measuring Sun-induced fluorescence in the oxygen absorption bands, *Biogeosciences*, *6*(7), 1181–1198.

Roháček, K., J. Soukupová, and M. Barták (2008), Chlorophyll fluorescence: A wonderful tool to study plant physiology and plant stress, in *Plant Cell Compartments-Selected Topics*, edited by B. Schoefs, pp. 41–104, Research Signpost, Kerala, India.

Rossini, M., M. Meroni, M. Migliavacca, G. Manca, S. Cogliati, L. Busetto, V. Picchi, A. Cescatti, G. Seufert, and R. Colombo (2010), High resolution field spectroscopy measurements for estimating gross ecosystem production in a rice field, *Agric. For. Meteorol.*, *150*(9), 1283–1296.

Rouse, J. W., R. H. Haas, J. A. Schell, D. W. Deering, and J. C. Harlan (1974), Monitoring the vernal advancements and retrogradation of natural vegetation, Final Report, NASA/GSFC Type III, 371 pp., Greenbelt, Md.

Ruban, A. V., D. Rees, A. A. Pascal, and P. Horton (1992), Mechanism of ΔpH-dependent dissipation of absorbed excitation energy by photosynthetic membranes. II. The relationship between LHCII aggregation in vitro and qE in isolated thylakoids, *Biochim. Biophys. Acta, Bioenerg.*, *1102*(1), 39–44.

Ruban, A. V., R. Berera, C. Ilioaia, I. H. M. van Stokkum, J. T. M. Kennis, A. A. Pascal, H. van Amerongen, B. Robert, P. Horton, and R. van Grondelle (2007), Identification of a mechanism of photoprotective energy dissipation in higher plants, *Nature*, *450*(7169), 575–578.

Schaepman-Strub, G., M. E. Schaepman, T. H. Painter, S. Dangel, and J. V. Martonchik (2006), Reflectance quantities in optical remote sensing-definitions and case studies, *Remote Sens. Environ.*, *103*(1), 27–42.

Van Rensen, J. J. S. (1989), Herbicides interacting with photosystem II, in *Herbicides and Plant Metabolism*, edited by A. D. Dodge, 21 pp., Cambridge Univ. Press, Cambridge, U. K.

Zarco-Tejada, P. J., V. Gonzalez-Dugo, and J. A. J. Berni (2012), Fluorescence, temperature and narrow-band indices acquired from a UAV platform for water stress detection using a micro-hyperspectral imager and a thermal camera, *Remote Sens. Environ.*, *117*, 322–337.